Electronic Supplementary Information

Systematic Investigation of an Array of TCNQ Lanthanide Complexes: Synthesis, Structure and Magnetic Properties

Juwen Zhang, Pengfei Yan, Guangming Li, Guangfeng Hou, Masayuki Suda and Yasuaki Einaga

Fig. S1 Perspective view for coordination geometry of La(III) ion in **1**.

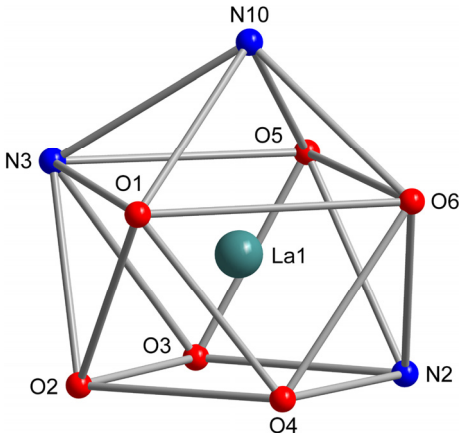

Fig. S2 Packing diagram of **1** viewed in the abb'a' plane (hydrogen atoms and interstitial solvents are removed for clarity).

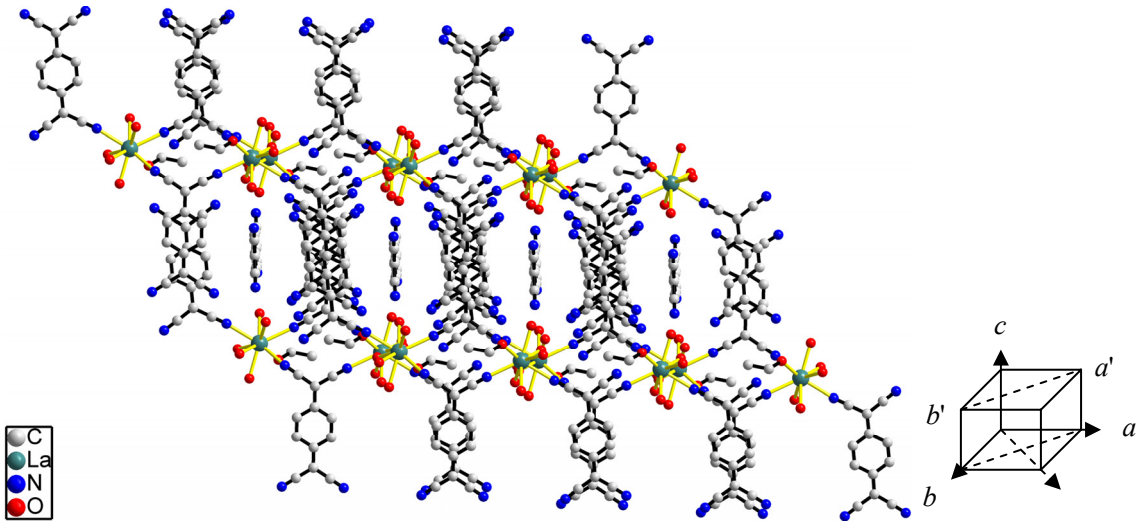

Fig. S3 Cationic structure of **3**. All hydrogen atoms are removed for clarity.

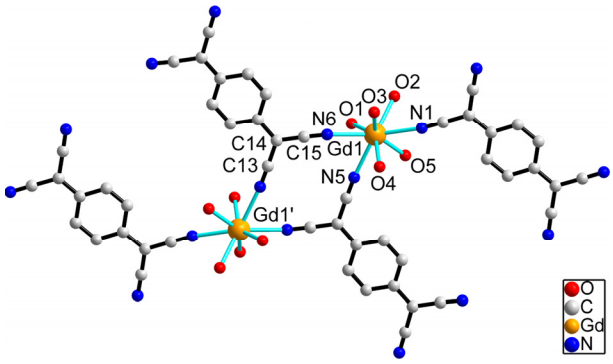

Fig. S4 Perspective view for coordination geometry of Gd(III) ion in **3**.

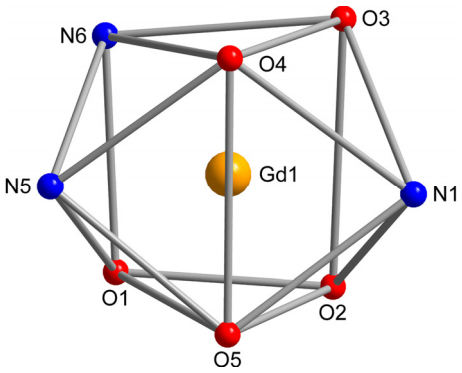

Fig. S5 Perspective view for coordination geometry of Er(III) ion in **5**.

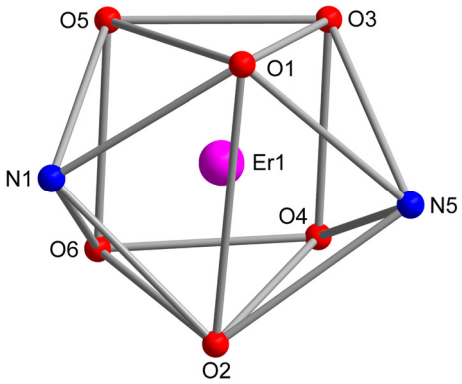

Fig. S6 Packing diagram of **5** viewed in the acc'a' plane (hydrogen atoms and interstitial solvents are removed for clarity).

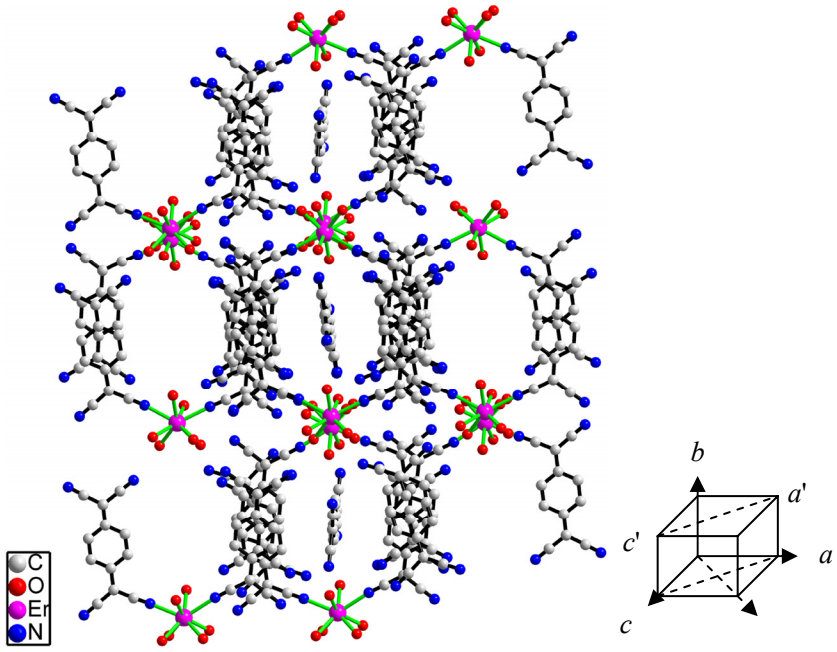

Fig. S7 Side view of the π-π stacking between $TCNQ^{\cdot -}$ radicals in **5**.

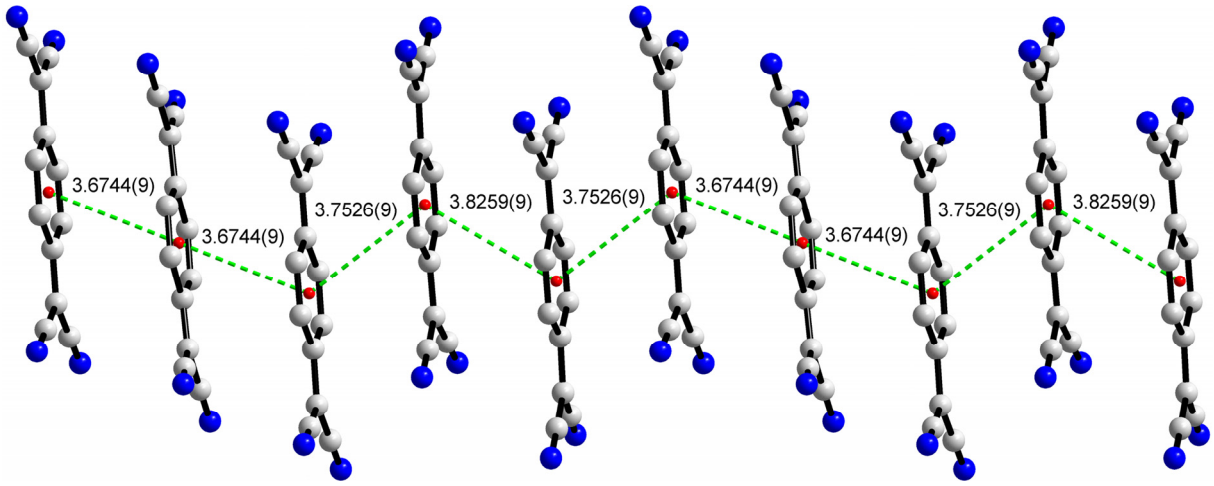

Fig. S8 Temperature dependences of $\chi_m T$ (**1** and **3**) and $\Delta\chi_m T = \chi_m T$ (**3**) $- \chi_m T$ (**1**).

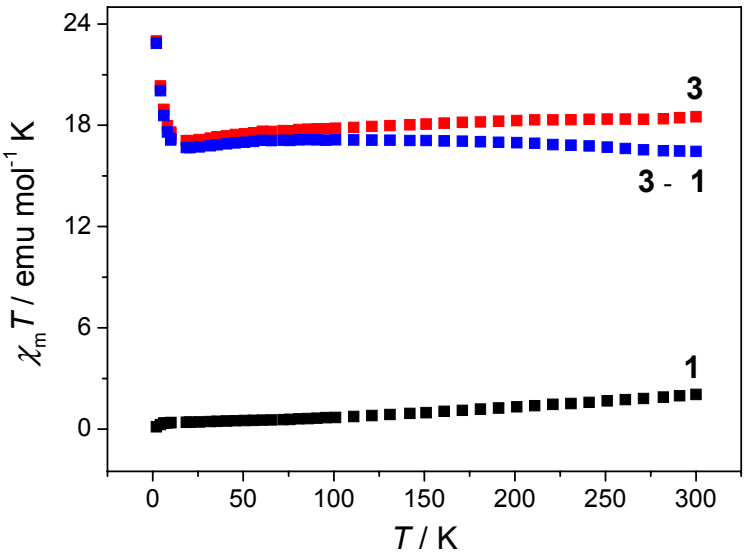

Fig. S9 Temperature dependence of AC susceptibility for **3**.

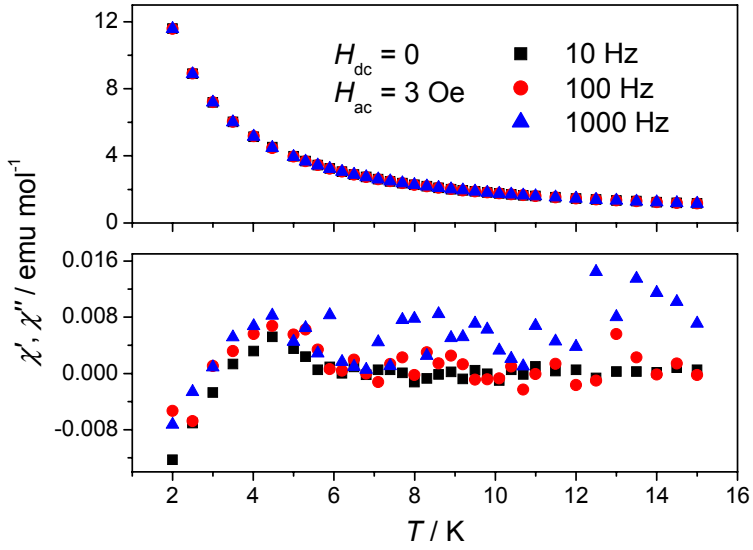

Fig. S10 Plots of FC and ZFC magnetization for **3** at 20 Oe.

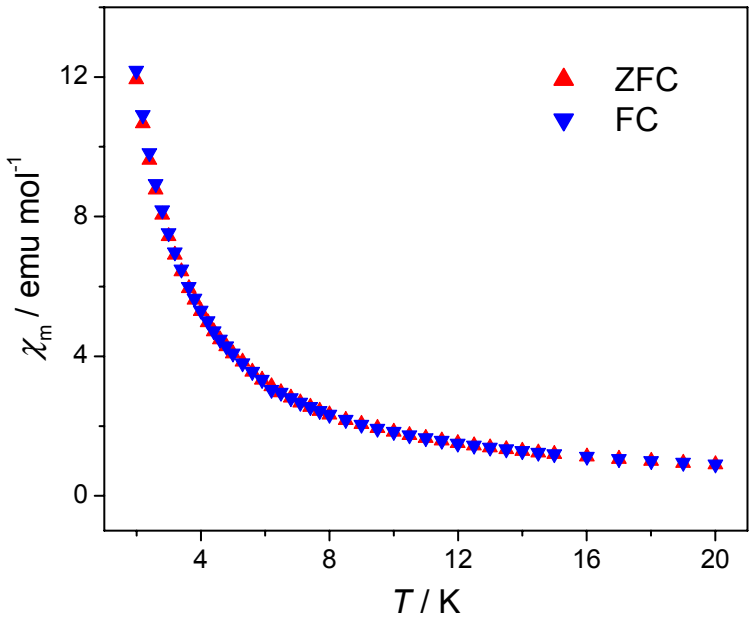

Fig. S11 *M* versus *H* plot for **3** at 2 K.

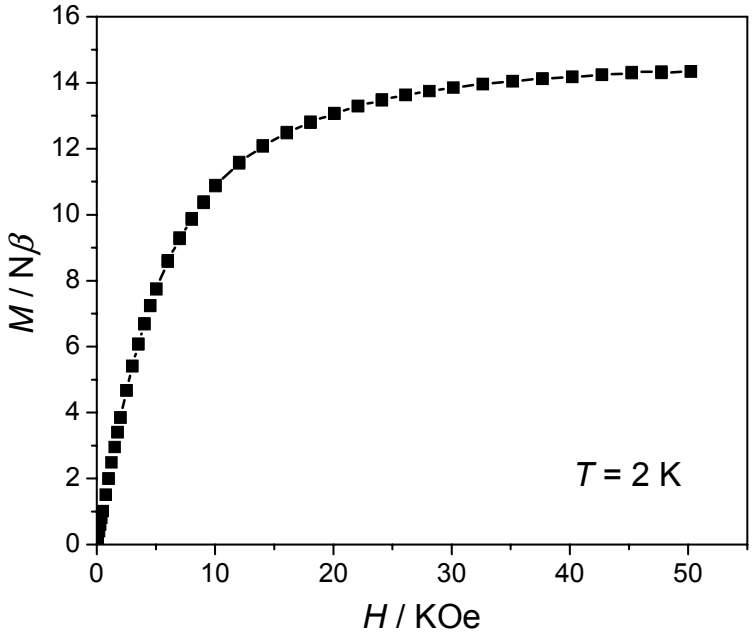

Fig. S12 TG (thermogravimetry) of **3** in N_2 atmosphere.

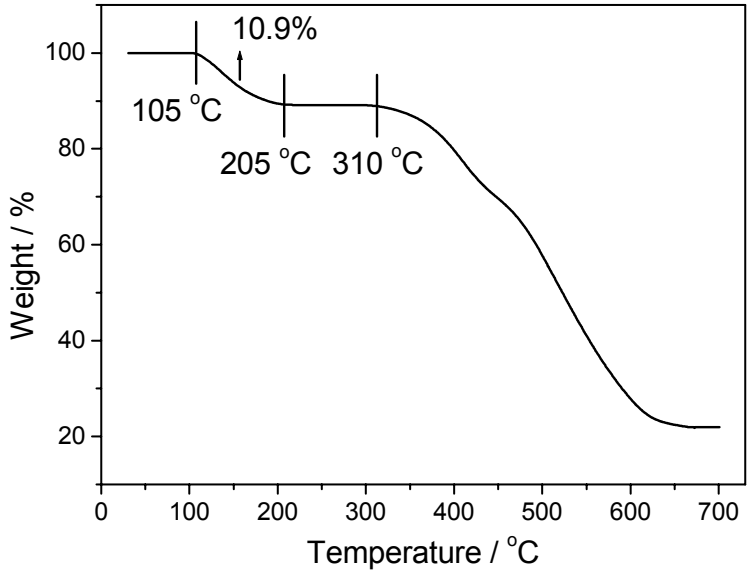

Fig. S13 *M* versus *H* plot for **3a** at 2 K.

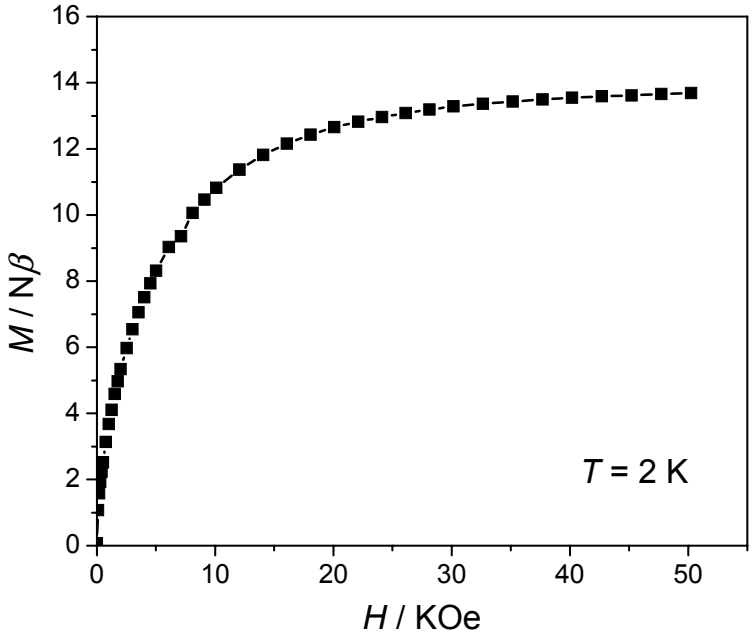

Fig. S14 *M* versus *H* loop for **3a** at 2 K.

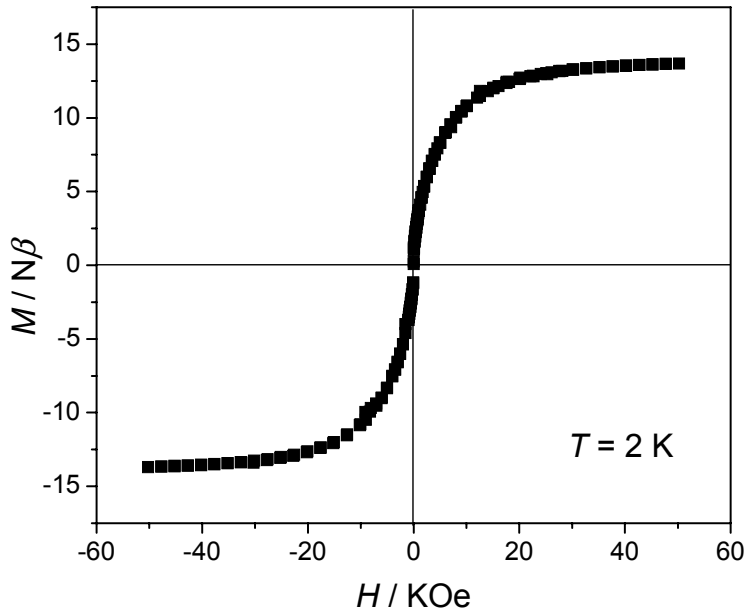

Fig. S15 X-ray powder diffraction pattern of **3a** (top) and simulated X-ray powder diffraction pattern of **3** (bottom).